

# Thirteen-Channel Wavelength Division Demultiplexer Based On Polymer Waveguide Holograms

Mark Peskin and Ray T. Chen

Microelectronics Research Center  
Department of Electrical and Computer Engineering  
University of Texas at Austin  
Austin, TX 78712

## Abstract

We present a thirteen-channel infrared wavelength division demultiplexer based on multiplexed phase-matched volume holograms recorded in a graded index (GRIN) polymer thin film waveguide. Channel center wavelengths ranged from 844 to 976 nm (11 nm channel separation), with corresponding output diffraction angles of  $22^\circ$  to  $70^\circ$  ( $4^\circ$  between channels). The device demonstrated diffraction efficiencies from 40% to 65% with an average channel crosstalk of -17.2 dB, which is largely attributable to the spectral width of the Ti:Al<sub>2</sub>O<sub>3</sub> laser source. The optical power requirements of the system are evaluated and shown to be well within practical limits.

## 1. Introduction

In motivating the transition from electrical to optical interconnection technologies, researchers frequently mention the enormous bandwidths of optical channels. Although multi-terahertz bandwidths are available in principle, in practice the light sources, modulators, and detectors necessary to transmit information on the optical channel are limited to speeds in gigahertz ranges. Therefore, in order to fully exploit the large bandwidth capability of optics, some form of multiplexing is necessary. In wavelength division multiplexing (WDM), the optical frequency space is effectively divided into segments, each of which is supported by its own modulator and detector, allowing a much larger total bandwidth to be employed than would otherwise be possible. The diffractive properties of optics allow WDM signals to be multiplexed and demultiplexed by completely passive optical elements. This is a key advantage of WDM over more conventional time division multiplexing techniques, which require an external clock signal.

Wavelength division multiplexing and demultiplexing (WD(D)M) devices have been fabricated using a number of different mechanisms, including optical interference filters<sup>1, 2</sup>, gratings<sup>3, 4</sup>, Mach-Zehnder interferometers<sup>5</sup>, and wavelength routers<sup>6</sup>. Currently, all of these designs exhibit shortcomings in channel crosstalk, spacing, or uniformity that tend to limit the number of channels that can be multiplexed. WD(D)M devices based on multiplexed holograms overcome many of these limitations (See Table 1). Each hologram is phase-matched to a single optical channel and, in the ideal case, does not interact with the other channels. This allows the characteristics of each demultiplexing hologram to be independently optimized for its channel. For example, the output orientation of each channel can be precisely controlled irrespective of channel wavelength. The number of holograms, and hence channels,

that can be multiplexed onto the same holographic emulsion for a given interaction length is limited only by the degree of index modulation that can be achieved in the grating region.

We present a thirteen-channel near infrared WD(D)M device based on highly multiplexed waveguide holograms fabricated in a graded index (GRIN) gel polymer thin film. Similar five-channel<sup>7</sup>, eight-channel<sup>8</sup>, and twelve-channel<sup>9</sup> near-IR devices have been previously reported. The graded index characteristic allows the film to serve as its own cladding, and the demultiplexing device can thus be directly fabricated on a large array of substrates<sup>10, 11</sup>.

## 2. Holographic Recording and Multiplexing

The device that we are reporting is designed to demultiplex thirteen channels from 844 to 976 nm, with 11 nm channel separation. Output channel diffraction angles ranged from 22° to 70° with 4° between adjacent channels. In order to calculate the proper phase matching condition for each channel, the dispersion characteristic of the polymer film,  $\bar{n}(\omega)$ , was determined within the channels' spectral range. The phase matching condition (See figure 1) demands that each hologram have a sinusoidal modulation profile and recording angle such that:

$$K_i = 2k_{\lambda_i} \sin\left(\frac{\theta_i}{2}\right) \quad (1)$$

where

$$k_{\lambda_i} = \bar{n}_i \frac{2\pi}{\lambda_{0_i}} \quad (2)$$

$$K_i = \frac{2\pi}{\Lambda_i} \quad (3)$$

- $\theta_i$  = angle of Bragg diffraction
- $\Lambda_i$  =  $i^{\text{th}}$  holographic grating period
- $K_i$  =  $i^{\text{th}}$  grating wave vector
- $k_{\lambda_i}$  =  $i^{\text{th}}$  signal wave vector
- $\bar{n}_i$  = effective index at  $\lambda_{0_i}$

In the polymer microstructure waveguide (PMSW) demultiplexer system, incident and refracted waves remain in the waveguiding plane, and the grating wave vectors are parallel to the waveguide surface. This significantly simplifies hologram recording geometry.

Holograms were recorded in a region of the PMSW that had been doped with a photoreactive compound—ammonium dichromate. Upon exposure to ultraviolet radiation, this sensitizing compound induces chemical crosslinking in the film, which in turn raises the refractive index in the crosslinked region<sup>12</sup>. Holographic gratings were recorded by coherent mixing of argon-ion laser beams, which were directed to set up a sinusoidally varying intensity pattern in the sensitized region. For each hologram to be recorded, two rotational recording angles,  $\phi_i$  and  $\omega_i$ , determine the values of  $\Lambda_i$  and  $\theta_i$ , respectively:

$$\varphi_i = \cos^{-1} \left( \frac{\lambda_R}{2\lambda_i} \right) \quad (4)$$

$$\omega_i = \frac{(\pi - \theta_i)}{2} \quad (5)$$

Here,  $\lambda_R$  is the wavelength of the recording beam in the PMSW medium. A recording system allowing precise control and modification of these angles was constructed for demultiplexer fabrication (See figure 2). In this system, the recording beam width is designed to be much larger than the holographic interaction length, thus ensuring that the recording beams are essentially planar in the interaction region.

An analysis based on Kogelnick's coupled wave theory for thick holograms leads to the following expression for the diffraction efficiency of a perfectly phase-matched, lossless, unslanted transmission grating:

$$\eta_i = \sin^2 \left( \frac{\pi \Delta n_i d}{\lambda_i \cos \theta_i} \xi \right), \quad (6)$$

where  $\Delta n_i$  is the refractive index modulation,  $d$  is the interaction length, and  $\xi$  is a constant that varies between 0 and 1 depending on the incident beam's polarization. The periodic dependence of  $\eta$  on  $\Delta n$  and  $d$  means that precise control of both recording geometry and exposure dosage is necessary to achieve large and uniform diffraction efficiencies across all channels, particularly for short wavelengths and large diffraction angles. Variations in diffraction angle and interaction length also affect the beamwidth of the output channels. This effect results in the channels with larger diffraction angles having larger beamwidths, which naturally tends to limit the spatial density of output channels that can be achieved without significant crosstalk. However, increasing the diffraction angle also increases the spectral selectivity, so design optimization is necessary in choosing diffraction angles<sup>13</sup>. If required, the output beams can be focused and collimated using waveguide lenses, which have already been successfully demonstrated in PMSW films<sup>14</sup>.

Precise control of  $\Delta n$  becomes more difficult as the number of channels, and hence the number of holograms to be multiplexed, is increased. This is due to the sensitized film's tendency to saturate after a finite exposure time, which results in a limiting index modulation value,  $\Delta n_{\max}$ . The refractive index of the sensitized PMSW film as a function of exposure dosage is plotted in figure 3. The exposure time necessary to induce an index modulation  $\Delta n_i$  for the  $i$ th exposure can be described by the following equation<sup>8</sup>:

$$t_i = \frac{1}{E\beta} \frac{\ln \left[ -\Delta n_i + \left( \Delta n_{\max} - \sum_{j=1}^{i-1} \Delta n_j \right) \right]}{\Delta n_{\max} - \sum_{j=1}^{i-1} \Delta n_j} \quad (7)$$

Here,  $\beta$  is a sensitivity constant for the photoactive region. Note that  $t_i$  increases as the number of holograms to be multiplexed increases. The finite  $\Delta n_{\max}$  of the sensitized PMSW also results in a

nonlinear relationship between exposure intensity and refractive index for long exposure times, resulting in harmonic distortion in the resulting grating profile<sup>15</sup> (See figure 4) which can potentially lead to coupling inefficiencies. In practice, these factors limit the number of holograms that can be multiplexed.

### 3. Results

The thirteen-channel device (See figure 5) was constructed in a PMSW thin film processed in a Class 100 clean room environment using a 1  $\mu\text{m}$  gel filtering process. This process produced a clean waveguide with low surface-scattering, and a propagation loss less than 0.1 dB/cm was observed. The refractive index of the PMSW film ( $\sim 1.5$ ) is compatible with high-index glass prisms ( $\sim 1.8$ ), which could therefore be used to efficiently couple light into and out of the waveguide. Observations of the well-collimated mode dots emerging from the sample at the various signal frequencies serve to confirm the quality of the waveguide as well as the effectiveness of the demultiplexing device (See figure 6). The high quality of the waveguide in which the WD(D)M device was constructed serves not only to reduce insertion losses but also to prevent potential crosstalk problems by minimizing inter-channel scattering and perturbations that might cause unwanted coupling between output channels.

Holograms were recorded using the process described above, yielding a multiplexed device with a 400  $\mu\text{m}$  interaction length. Note that this interaction length, and thus the amount of "real-estate" required by our device, is quite small in comparison to the other WD(D)M devices mentioned above. Input channels with center wavelengths of 844, 855, 866, 877, 888, 899, 910, 921, 932, 943, 954, 965, and 976 nm were excited using a Ti:Al<sub>2</sub>O<sub>3</sub> laser. Diffraction efficiencies from 40% to 65% were measured, with an average channel crosstalk of -17.2 dB. The spectral width of the Ti:Al<sub>2</sub>O<sub>3</sub> laser was subsequently evaluated. A FWHM of  $\sim 4$  nm was found, together with a bandwidth of  $\sim 11$  nm at -30 dB. It is clear that the wavelength spreading of the Ti:Al<sub>2</sub>O<sub>3</sub> laser source is largely responsible for the measured channel crosstalk. Reducing detector sensitivity can hide this crosstalk, but only at the expense of system power budget requirements. Use of a narrow bandwidth light source, such as a DFB laser diode, should reduce crosstalk drastically and may permit spectral channel spacing of 1 nm or less.

### 4. WDDM System Considerations

In order to evaluate the potential of our WD(D)M device for real world applications, the power budget requirements must be calculated. Since the channels assumed to be driven by separate sources, the power budget can be calculated independently for each channel. For a 10 Gbit/sec channel, we would expect a bit error rate (BER) less than  $10^{-10}$ , which translates into a detector S/N ratio ( $i_s/\langle i_N \rangle$ ) of 12.86 (25.54 dB), assuming the relationship<sup>16</sup>:

$$\text{BER} = \frac{1}{2} \operatorname{erfc} \left( \frac{i_s}{2\sqrt{2} \langle i_N \rangle} \right) \quad (8)$$

There is a well known relationship between detector S/N ratio and optical power incident on the detector ( $P_s$ ):

$$\frac{i_s}{\langle i_N \rangle} = \frac{P_s e \eta / h \nu}{(4kT_e \Delta \nu / R_l)^{1/2}} \quad (9)$$

If we assume a channel center wavelength of 800 nm, a 25.54 dB S/N ratio, and typical values for the detector system, we can use Eq. (9) to calculate a minimum required optical signal power at the detector of 0.28 mW. If we make the following assumptions, which are conservative based on the performance of our test sample:

Hologram diffraction efficiency	$\eta_d = 50\%$
Hologram excess loss	$L_H = -2$ dB
Waveguide coupling loss	$L_c = -3$ dB
Waveguide propagation loss	$\alpha = -1$ dB/cm
Waveguide propagation length	$\ell = 5$ cm

then the minimum required power for each channel ( $P_i$ ) can be calculated by

$$10 \log\left(\frac{P_s}{\eta_d P_i}\right) = L_c + L_H + \alpha \ell \quad (10)$$

This yields  $P_i = 1.5$  mW. With a 5 dB system power margin, this translates into a required laser input power of 2.5 mW per channel, which is well within the capabilities of commercial laser diodes.

The finite index modulation depth ( $\Delta n_{\max}$ ) of the PMSW film means that more channels can be multiplexed if the index modulation associated with each hologram ( $\Delta n$ ) is reduced. However, according to Eq. (6), reductions in  $\Delta n$  also reduce the hologram diffraction efficiency. Thus, there is clearly a tradeoff between the number of channels ( $N$ ) and system power requirements. This relationship can be summarized as follows (for small to moderate diffraction efficiencies):

$$P_i \propto \frac{1}{\eta_d} \propto \frac{1}{\Delta n^2} \propto N^2 \quad (11)$$

Future refinements in materials or processing techniques may lead to increases in  $\Delta n_{\max}$ , together with reductions in coupling, propagation, and excess losses. This will lead to decreased system power requirements and/or larger numbers of available channels.

## 5. Conclusion

We have successfully demonstrated a thirteen-channel infrared WD(D)M device based on multiplexed volume holograms optically recorded in a sensitized polymer microstructure waveguide. Channel center wavelengths ranged from 844 to 976 nm (11 nm channel separation), with corresponding output diffraction angles of 22° to 70° (4° between channels). The completed device demonstrated diffraction efficiencies from 40% to 65% with an average channel crosstalk of -17.2 dB. This crosstalk value is largely attributable to the spectral characteristics of the Ti:Al<sub>2</sub>O<sub>3</sub> laser used as an input source, and substantial improvements in this figure should be attainable using narrow bandwidth laser sources. Optical power requirements of the holographic system have been estimated and shown to be well within the capabilities of commercially available semiconductor lasers. There is a tradeoff between system power requirements and the number of multiplexed channels, which is limited by the maximum index modulation depth of the PMSW film. However, refinements in materials and processing are expected to reduce the severity of these restrictions.

Wavelength division multiplexing techniques can enhance the bandwidth of optical interconnection systems enormously. The multiplexed holographic WD(D)M is superior to other designs in terms of its ability to efficiently handle a large number of channels over a large frequency range with high efficiency and low crosstalk. The GRIN PMSW film in which the device is fabricated is inexpensive, easy to process, and can be used to form high-quality waveguides on any substrate of interest without the added complexity of a buffer layer. This leads to a great degree of system flexibility. Together with the demonstrated performance of this device, these considerations make the polymer holographic WD(D)M a promising and practical candidate for applications in future optical interconnection systems.

## 6. References

1. Bennion, I., *et al.*, *High Reflectivity Monomode-Fibre Grating Filters*. Electronics Letters, 1986. 22(6): pp. 341-343.
2. Sorin, W.V., P. Zorabedian, and S.A. Newton, *Tunable Single-Mode Fiber Reflective Grating Filter*. IEEE Journal of Lightwave Technology, 1987. LT-5(9): pp. 1199-1202.
3. Fujii, Y., J. Minowa, and Y. Yamada, *Optical Demultiplexer Utilizing an Ebert Mounting Silicon Grating*. IEEE Journal of Lightwave Technology, 1984. LT-2(5): pp. 731-734.
4. Ura, S., *et al.*, *Integrated Optic Wavelength Demultiplexer Using a Coplanar Grating Lens*. Applied Optics, 1990. 29(9): pp. 1369-1373.
5. Verbeek, B.H., *et al.*, *Integrated Four-Channel Mach-Zehnder Multi/Demultiplexer Fabricated with Phosphorous Doped SiO<sub>2</sub> Waveguides on Si*. IEEE Journal of Lightwave Technology, 1988. 6(6): pp. 1011-1015.
6. Zirngibl, M., *Fabrication of Optical Splitters and Wavelength Routers Using InP-Technology*. Optics & Photonics News, 1993. March: pp. 27-29.
7. Wang, M.R., *et al.*, *Five-Channel Polymer Waveguide Wavelength Division Demultiplexer for the Near Infrared*. IEEE Photonics Technology Letters, 1991. 3(1): pp. 36-38.
8. Chen, R.T., *et al.*, *Highly Multiplexed Graded-Index Polymer Waveguide Hologram for Near-Infrared Eight-Channel Wavelength Division Demultiplexing*. Applied Physics Letters, 1991. 59(10): pp. 1144-1146.
9. Chen, R.T., *Polymer-based Passive and Active Guided-wave Devices and Their Applications*, in *Critical Reviews*. 1992, pp. 198-235.
10. Chen, R.T., *et al.*, *Integration of Holographic Optical Elements with Polymer Gelatin Waveguides on GaAs, LiNbO<sub>3</sub>, glass, and aluminum*. Optics Letters, 1989. 14(16): pp. 892-894.
11. Chen, R.T., M.R. Wang, and T. Jansson, *Polymer Microstructure Waveguides on Alumina and Beryllium Oxide Substrates for Optical Interconnection*. Applied Physics Letters, 1990. 56(8): pp. 709-711.
12. Beeson, K.W., *et al.* *Polymeric Materials for Guided-Wave Devices*. 1990. Proceedings of the SPIE, Vol. 1337.
13. Chen, R.T. *Polymer Gelatin Microstructure Waveguides In Conjunction With HOE For Electronics and VLSI Optical Interconnects*. 1992. Final Report to U. S. Army Strategic Defense Command: DASG60-90-C-0018.
14. Chen, R.T. 1991. Final Report to Army Harry Diamond Lab: DAAL02-91-C-0034.
15. Jansson, T., G. Savant, and Y. Qiao. *Holographic Rugate Structures For X-ray Optics Applications*. 1988. Annual Report to U. S. Department of Energy: AR-DOE-080188.
16. Yariv, A. and P. Yeh, *Optical Waves in Crystals*. 1st ed. 1984, New York: John Wiley & Sons. p. 589.

Device	Advantages	Disadvantages	Large Number of Channels Impractical
<b>Optical Interference Filters</b>	<ul style="list-style-type: none"> <li>• Simplicity</li> <li>• Very low crosstalk possible</li> </ul>	<ul style="list-style-type: none"> <li>• Bulky</li> <li>• Difficult to align</li> <li>• Lossy</li> </ul>	
<b>Gratings</b>	<ul style="list-style-type: none"> <li>• Simplicity</li> </ul>	<ul style="list-style-type: none"> <li>• Difficult to align</li> <li>• Crosstalk levels unacceptable</li> </ul>	
<b>Mach Zehnder Interferometers</b>	<ul style="list-style-type: none"> <li>• Easy to integrate</li> <li>• Low crosstalk possible</li> <li>• Small channel spacing possible</li> </ul>	<ul style="list-style-type: none"> <li>• Large interaction length</li> <li>• Bandwidth usage limited</li> <li>• Channel spacing not flexible</li> </ul>	
<b>Wavelength Routers</b>	<ul style="list-style-type: none"> <li>• Easy to integrate</li> <li>• Crosstalk acceptable</li> <li>• Larger number of channels than above designs</li> </ul>	<ul style="list-style-type: none"> <li>• Channel uniformity poor, especially for large number of channels</li> </ul>	
<b>Multiplexed Holograms</b>	<ul style="list-style-type: none"> <li>• Large number of channels</li> <li>• Short interaction length</li> <li>• Channel uniformity, geometry, and wavelength easily controllable</li> <li>• Very low crosstalk possible</li> </ul>	<ul style="list-style-type: none"> <li>• Strict channel number/power budget tradeoff</li> </ul>	

Table 1 : Comparison of various demonstrated WD(D)M devices.

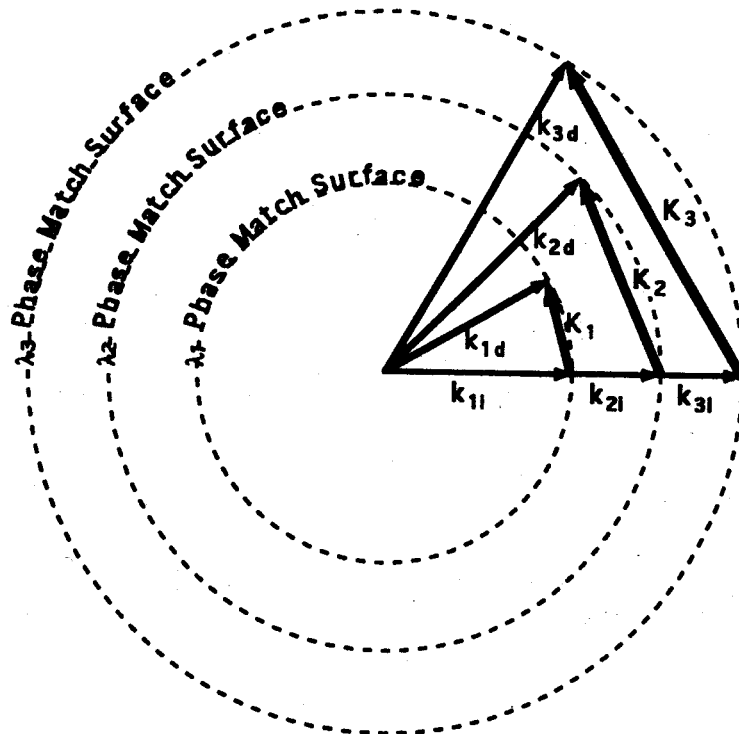


Figure 1 : Ring diagram showing phase matching condition in holographic WDDM.

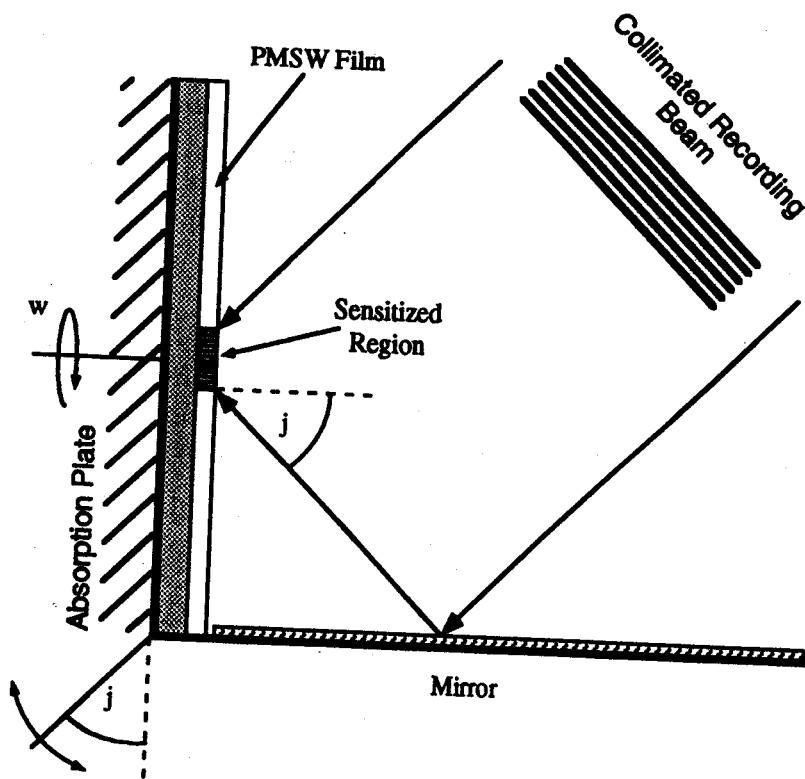


Figure 2 : Schematic of hologram recording stage.

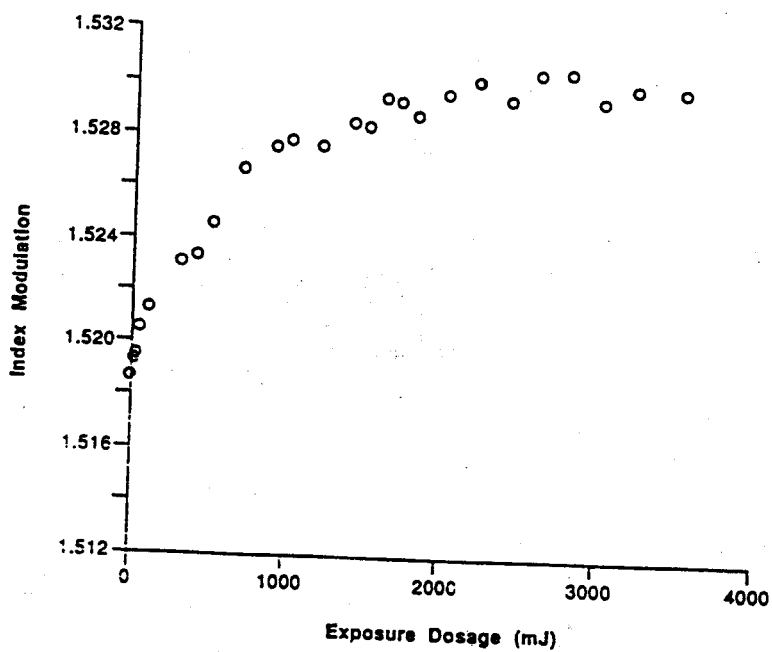


Figure 3 : Index modulation versus exposure dosage in sensitized PMSW film.



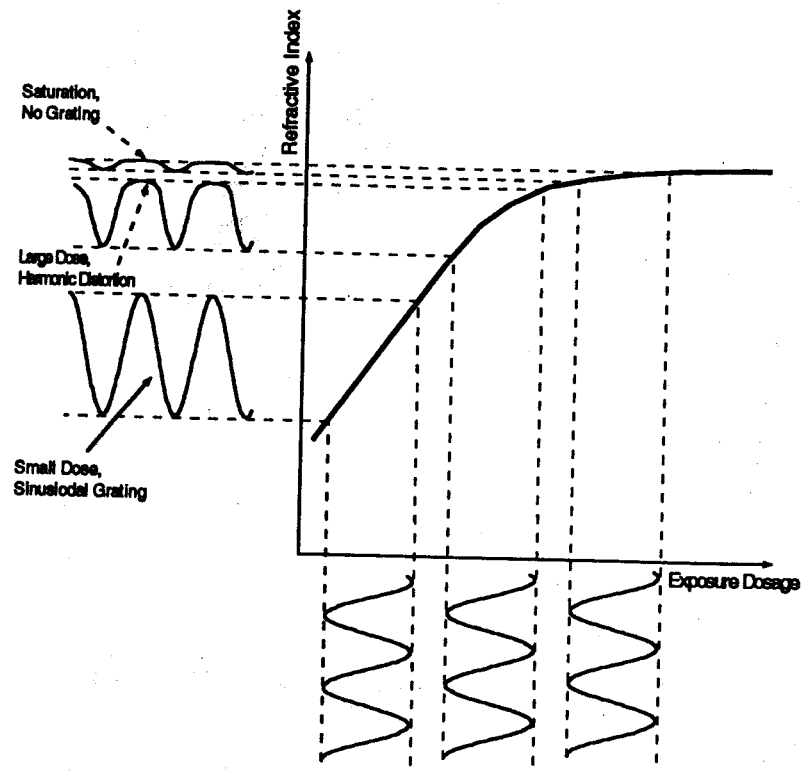


Figure 4 : Effects of holographic film saturation on grating profile.

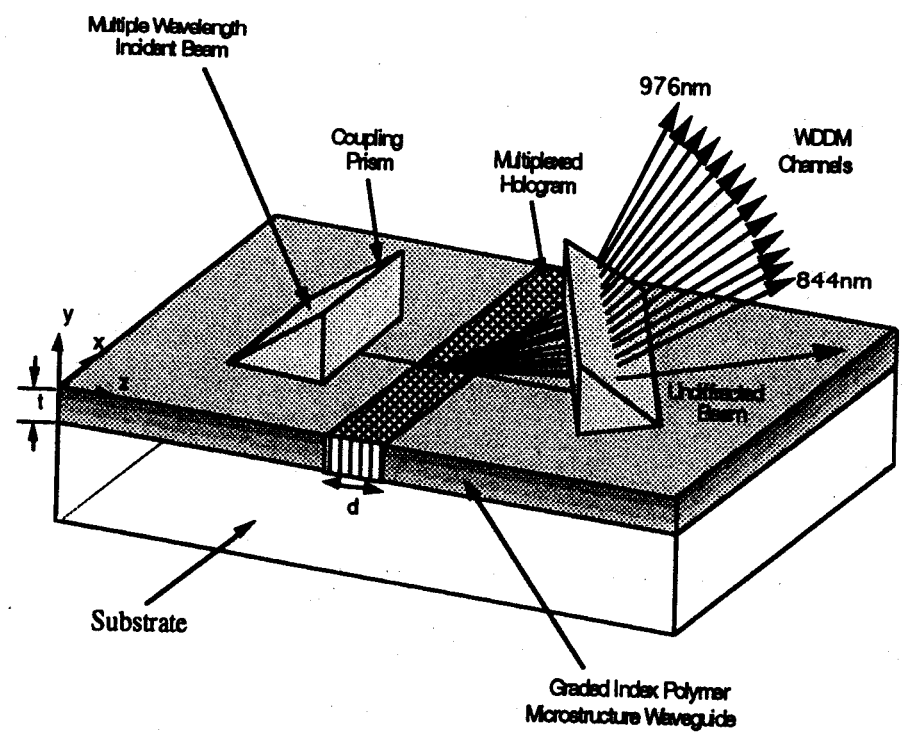


Figure 5 : Schematic of completed device showing prism couplers.

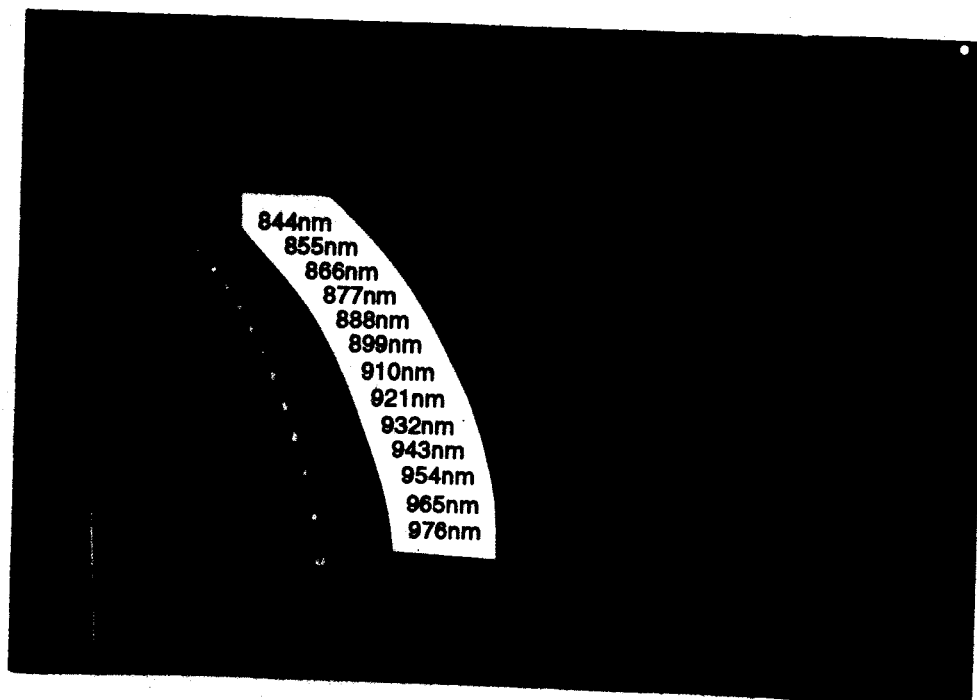


Figure 6 : Photograph of mode output dots from completed device showing 13 channel separation (taken with Vidicon IR camera).